Dynamic correlations in a dense dipolar liquid

J. Dawidowski,[1] A. Chahid,[2] F. J. Bermejo,[1] E. Enciso,[3] and N. G. Almarza[3]

[1] *Instituto de Estructura de la Materia, Consejo Superior de Investigaciones Cientificas, Serrano 123, E-28006 Madrid, Spain*

[2] *Departamento de Física de Materiales, Universidad del País Vasco, P.O. Box 1072, E-20080 San Sebastián, Spain*

[3] *Departamento de Química-Física I, Facultad de Ciencias Químicas, Universidad Complutense, Ciudad Universitaria, E-28040 Madrid, Spain*

(Received 6 April 1995)

The microscopic dynamics of liquid sulphur dioxide is investigated by means of the concurrent use of inelastic neutron scattering and molecular dynamics simulations. This enables an approximate separation of the dynamic processes contributing to the neutron spectra, thus allowing us to quantify the deviation from idealized behavior of quantities characterizing the single-particle and collective motions. From a comparison between experiment and simulation, an estimate of an inelastic structure factor comprising information about the extent of orientational correlations is derived. Finally, the relevance of the present results as benchmarks to assess recent predictions is discussed.

PACS number(s): 61.25.Em, 71.20.Fi, 61.20.Lc

I. INTRODUCTION

Because of the highly directional nature of the interparticle interactions, the dynamical response of a dense dipolar fluid is expected to exhibit properties remarkably different from simple (i.e., Lennard-Jones) liquids. Particularly appealing were the suggestions of Lobo *et al.* [1] and Pollock and Alder [2], stating the existence of collective oscillations in the longitudinal component of the polarization function, termed dipolarons thereinafter, in analogy with the plasma oscillations in Coulomb systems. Such excitations were found to be the origin of the strong dynamic correlations between dipolar particles [3], as they also have a remarkable role in explaining some anomalies in the shear or rotational viscosities of such a class of fluids [4]. Although the theoretical constructs dealing with microscopic scales still show some consistency problems (i.e., the continuum limit of those approaches is in some cases lacking, although attempts within the framework of extended irreversible thermodynamics [4] seem to provide a way of linking these efforts with the more elaborate macroscopic treatments; see Ref. [5] as an example), the fact that some computer molecular dynamics results in point dipoles or calculations for realistic systems [6] have proven the existence of such oscillations [2] has led to a number of efforts trying to detect such phenomena in real systems [7]. The experimental verification of such predictions has, however, encountered a number of difficulties as a consequence of the need to fulfill some stringent conditions regarding the microscopic time scales adequate for the appearance of non-over-damped responses in the longitudinal component of the $\vec{\epsilon}(Q,\omega)$ dielectric tensor. However, because the coupling between polarization fluctuations and hydrodynamic modes provides effective channels for the dissipation of dielectric energy, it is expected that a number of microscopic properties of these fluids, especially those related to hydrodynamic flow (viscosities) and angular velocity (single-particle rotations), will also show some anomalous behavior.

A number of attempts to explore the extent of orientational correlations in liquids formed by particles carrying permanent dipole moments have also appeared in recent times [8]. In particular, some recent findings regarding a somewhat more realistic fluid, formed by particles interacting via dipolar and dispersion forces [9], has reported the existence of a variety of critical phenomena depending upon the particle aspect ratio. Even if such findings are only qualitative, due to the oversimplified form of representing realistic molecular interactions, some of the predictions already made, such as the presence of long-ranged correlations of molecular orientations, seem worth contrasting against experimental or simulational data.

The purpose of the present work is thus to provide an assessment of the nonideal behavior of several microscopic dynamical quantities on a real fluid, sulphur dioxide, by means of the study of the stochastic (low-frequency) motions as sampled by quasielastic neutron scattering (QENS) measurements. Because of the limited information directly available from the QENS spectra of classical liquids, the analysis of the experimental intensities has been carried out by recourse to functions calculated by means of computer molecular dynamics simulations, which has enabled the derivation of extremely useful microscopic information hardly available from other means. As described below, the computer simulation results will serve to separate the different atomic motions contributing to the experimental spectra and constitute a benchmark that allows one to overcome some inadequacies of the simulation results. The choice of such a liquid was motivated by its simple structure (i.e., far more simple than other liquids recently examined such as liquid water [6]), which allows simulations to be carried on realistic model potentials, and easiness of handling, as well as by the amount of information already available concerning static correlations [10], collective dynamics [11], and elastic properties [12].

II. EXPERIMENTAL AND COMPUTATIONAL DETAILS

The neutron experiment was performed on the IN6 spectrometer located at the Institut Laue Langevin (ILL) (Grenoble, France). The cylindrical cell (10 mm diameter, 50 mm height) was filled with the liquid under saturated vapor pressure. In order to reduce the contribution of the multiply scattered neutrons, the cell contained five cadmium spacers 0.3 mm thick placed parallel to the beam direction. The sample was measured at temperatures of 190, 210, and 230 K and the transmission geometry ($\alpha = 135°$) was employed. We used an incident wavelength of 4.1 Å, corresponding to an energy of about 4.87 meV and the resolution was better than 0.1 meV. The spectra were corrected by standard ILL programs for detector efficiency, sample container, absorption, and self-shielding. The dynamical structure factor $S(Q,\omega)$ was then converted to constant Q with the INGRID computer code. In agreement with previous findings regarding the microscopic structure of the fluid, the main differences between data sets corresponding to different temperatures could easily be explained in terms of the concomitant change in density, so that the ensuing discussion will only concern one thermodynamic state. A set of spectra taken at different values of the momentum transfer is shown in Fig. 1.

Molecular dynamics simulations on the system at several temperatures were performed, although only data at 230 K will be discussed for reasons mentioned above. In each run a cubic simulation cell containing 256 molecules has been used. The equations of motion have been solved by applying the Gear predictor-corrector method. The integration time step was 10^{-15} s and a typical run was about 30 000 time steps giving a simulation length of 30 ps. This has been done to ensure that the incoherent intermediate function vanishes at long times. The intermolecular potential used was a three-site Lennard-Jones model with electric point charges that corresponds to the thermodynamic state 4 of model C proposed by Sokolić *et al.* [13]. The relevant parameters regarding the interaction forces are summarized in Table I, and the charge interactions were handled by means of the standard Ewald summation procedure.

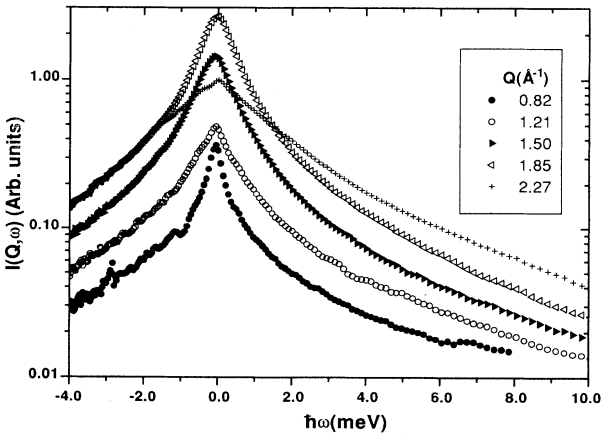

FIG. 1. Experimental, constant-Q spectra for different values of the momentum transfer given in the inset.

TABLE I. Thermodynamic and potential energy parameters for the molecular dynamics simulation. L stands for the side of the simulation box, $d_{\alpha-\beta}$ are the bond lengths, r_{cutoff} represents the cutoff radius for the electrostatic interactions, and the rest of the symbols retain their usual meaning. Electrostatic point charges q_i are expressed in units of the electron charge.

Parameter	Value
T (K)	230
ρ (Kg/m^3)	1.541×10^3
L (Å)	26.05
d_{S-O} (Å)	1.434
d_{O-O} (Å)	2.47
r_{cutoff} (Å)	13
q_S (e)	0.47
q_O (e)	−0.235
σ_{S-S} (Å)	3.610
σ_{O-O} (Å)	3.000
ϵ_{S-S}/k_B (K)	146
ϵ_{O-O}/k_B (K)	57.5

Some computations regarding static quantities were also carried out by means of a Monte Carlo code [14]. For this calculation a cubic simulation cell, with sides of 27.75 Å, containing 256 molecules interacting through the potential described in Table I was used. The potential was truncated using a cutoff radius of 10 Å. The total number of steps was of 1 600 000 from which 800 000 corresponded to translational motion (256 156 were accepted) and 800 000 to rotations (292 757 accepted). The same thermodynamic states explored in a previous work [10], that is, temperatures of 190, 210, and 230 K, were simulated.

III. RESULTS

The complete double differential scattering cross section can be written

$$\frac{d^2\sigma}{d\Omega d\omega} = \frac{k}{k_0}\frac{1}{2\pi}\int_{-\infty}^{\infty} e^{-i\omega t}\,\sigma(\mathbf{Q},t)\,dt, \tag{1}$$

in which the intermediate scattering function $\sigma(\mathbf{Q},t)$ can be separated in inter- and intramolecular parts and the wave vector expressed in terms of its modulus due to the isotropy condition

$$\sigma(Q,t) = I_d(Q,t)\,F_2(Q) + I_s(Q,t)\,v(Q,t). \tag{2}$$

The position of the νth nucleus in the jth molecule can be written as

$$\boldsymbol{R}_{j\nu} = R_j + r_{j\nu}, \tag{3}$$

where $\boldsymbol{R}_j$ is the jth molecule's position of the center of mass and $\mathbf{r}_{j\nu}$ is the position of atom ν in molecule j with respect to its center of mass.

As usual, we define the distinct and self-parts of the

intermediate scattering function as

$$I_d(Q,t) = \sum_{i \neq j} \left\langle e^{-i\mathbf{Q}\cdot\mathbf{R}_i(0)}\, e^{i\mathbf{Q}\cdot\mathbf{R}_j(t)} \right\rangle \tag{4}$$

and

$$I_s(Q,t) = \sum_{i} \left\langle e^{-i\mathbf{Q}\cdot\mathbf{R}_i(0)}\, e^{i\mathbf{Q}\cdot\mathbf{R}_i(t)} \right\rangle, \tag{5}$$

respectively. The term $F_2(Q)$ appearing in Eq. (2) is an intermolecular form factor, which obviously depends upon the correlation of the molecular orientations [15] and can be written in general terms as

$$F_2(Q) = \left\langle \sum_{\mu_i,\nu_j} b_{\mu_i} b_{\nu_j} e^{i\mathbf{Q}\cdot(\mathbf{r}_{\nu j} - \mathbf{r}_{\mu i})} \right\rangle. \tag{6}$$

Notice that the quantity given above contains relevant physical information from which estimates of a correlation length could be derived. Finally, the function $v(Q,t)$ encompasses the molecular, single-particle reorientational motions and can be expressed as a partial-wave expansion [16]

$$v(Q,t) = \sum_{l=0}^{\infty} v_l(Q)\, F_l(t), \tag{7}$$

$$v_l(Q) = (2l+1) \sum_{\mu,\nu} (b_{\mu,\mathrm{coh}} b_{\nu,\mathrm{coh}} + b^2_{\mu,\mathrm{inc}} \delta_{\mu\nu}) \times j_l(Q r_\mu)\, j_l(Q r_\nu)\, P_l[\cos(\theta_{\mu\nu})], \tag{8}$$

in which $F_l(t)$ are the rotational relaxation functions, j_l are the spherical Bessel functions, P_l are the Legendre polynomials, and $\theta_{\mu\nu}$ is the angle between vectors $\mathbf{r}_{j\mu}$ and $\mathbf{r}_{j\nu}$. The subscripts "coh" and "inc" denote the coherent and incoherent scattering lengths, respectively. The latter functions will thus contain all the relevant dynamics regarding stochastic molecular rotations; one of the main objectives of the present simulation was to explore the extent of departure of such functions from idealized Debye behavior (i.e., simple exponential relaxation).

In the limit of low-Q values it is sufficient to consider only up to the term l=2 in the above expansion (cf. Ref. [16]). In the rest of this work we will neglect the higher-order terms.

Each one of these components, i.e., $I_d(Q,t)$, $I_s(Q,t), v(Q,t)$, and $F_l(t)$, was modeled on the basis of those correlation functions calculated by means of molecular dynamics simulations. The modeling was performed on the Q-ω space, i.e., the time Fourier transform of the above shown quantities, and the most relevant details are given below.

A. Self-scattering law

Attempts to describe the self-component $I_s(Q,t)$ with a simplified function failed, as none of the feasible forms of joining the short-time, basically Gaussian, behavior and long time (diffusional) regimes was found to reproduce the calculated functions. The latter showed a typical exponential decay with a clear quadratic dependence on the wave vector, while at short times a free translation regime dominated. To interpolate between these two regimes we adopted a three-pole formula [17], which has proven to be an adequate means of describing the time Fourier transform $S_{\mathrm{self}}(Q,\omega)$ while preserving the second and fourth moments of the dynamical structure factor for single-particle motions. The self, dynamic structure factor thus reads

$$S_{\mathrm{self}}(Q,\omega) = \frac{\tau\omega_0^2(\omega_s^2 - \omega_0^2)}{[\omega\tau(\omega^2 - \omega_s^2)]^2 + [(\omega^2 - \omega_0^2)]^2}, \tag{9}$$

where the relaxation time is evaluated following a simple approximation, which leads to

$$\tau = \frac{k_B T}{m D \Omega_0} \frac{1}{\sqrt{\omega_s^2 - \omega_0^2}}. \tag{10}$$

Ω_0 represents some vibration frequency of a molecule in the liquid if the rest is maintained at its equilibrium position [18]

$$\Omega_0^2 = \omega_s^2 - 3\omega_0^2 \tag{11}$$

and ω_0 and ω_s are related to the reduced second and fourth frequency moments of the scattering function as

$$\omega_0^2 = \langle \omega^2 \rangle = \frac{Q^2}{M_{\mathrm{mol}}\beta}, \tag{12}$$

$$\omega_s^2 = \frac{\langle \omega^4 \rangle}{\langle \omega^2 \rangle}, \tag{13}$$

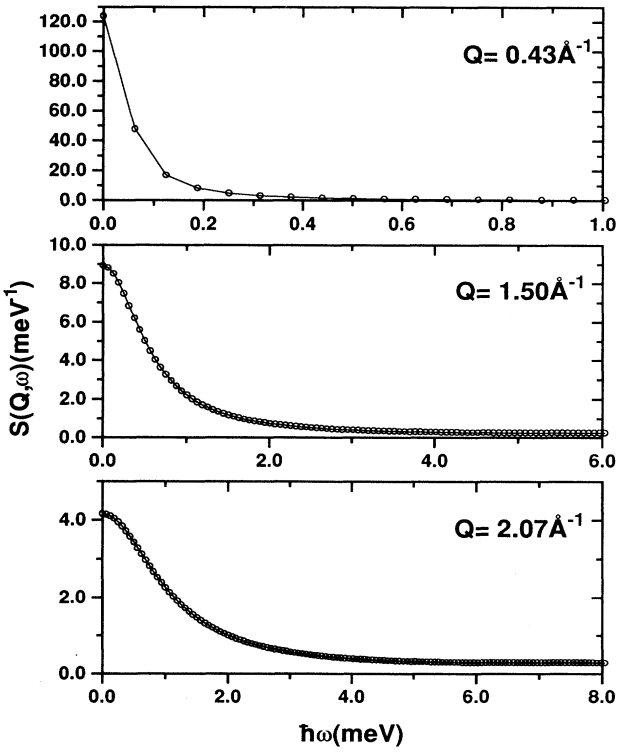

FIG. 2. Self-scattering function from simulation (circles), compared with the fitted three-pole model, for two different Q values.

with $\beta = 1/k_B T$ and M_{mol} being a molecular mass. A good fit between the simulation and this model was achieved (as shown in Fig. 2 for three different Q values), although a rather small value for the self-diffusion constant was observed (0.8×10^{-9} m^2 s^{-1}). The reasons for this are both the small size of the simulation box employed, which cannot take account of the large distances implied in the diffusional regime, as well as possible inadequacies of the interparticle potential. An estimate of the translational diffusion coefficient of the liquid was, on the other hand, obtained from a Lorentzian fit over the low-Q values of the experimental spectra (0.24–0.66 Å^{-1}), which gave the value 4.45×10^{-9} m^2 s^{-1} for the diffusion constant, which was adopted in the further analysis. The reason for the failure of any simple model to account for the spectral shape can be gauged from the values of the parameter [19]

$$\alpha = \frac{\langle \omega^4 \rangle}{3 \langle \omega^2 \rangle^2} - 1, \tag{14}$$

which is zero for a Gaussian form and infinite for a Lorentzian form. In Fig. 3 we show the α values for different Q's and a transition between the Lorentzian (Fickian diffusion) regime and a Gaussian can be observed at $Q \simeq 0.5$ Å^{-1}, although full Gaussian behavior seems to be confined to wave vectors above 2 Å^{-1}. Within the inset of the same figure, we show the fitted values for ω_0 and ω_s. The slope of ω_0 versus wave vector gives a value for the effective mass for single-particle motion, which turns out to be approximately equal to 101 amu, which is about 1.57 times the mass of the isolated molecule, and the estimated Ω_0 characteristic frequency approximately equal to 3 meV, a value difficult to correlate with any distinctive feature appearing in the experimental $Z(\omega)$ generalized frequency distribution shown in Fig. 3a of Ref. [12].

B. Rotational relaxation functions

Since the orientational correlations are supposed to be strong, it can be expected that the rotational motion of the SO_2 molecule substantially deviates from simple (small step) diffusional movement. In fact, as shown by Wasylishen *et al.* [21] in a ^{33}S and ^{17}O NMR study, such a departure is expected to occur since the free-rotational time is of the same order as the mean time between collisions. For this reason a simple exponential behavior cannot describe the rotational relaxation functions. In order to account for this, several different possibilities were explored. From those, the most adequate model to describe the rotational relaxation functions was that due to Larsson and Bergstedt [22], in which it is supposed that the molecule exists in two phases of rotational motion: either free rotation during an average time τ_0 or rotational diffusion during time τ_1. The corresponding equations for $F_l(t)$ in these two states are, respectively,

$$F_{l,\text{free}}(t) = \exp\left[-l(l+1)\frac{k_B T}{2I} t^2\right], \tag{15}$$

$$F_{l,\text{diff}}(t) = \exp\left[-l(l+1) D_R |t|\right], \tag{16}$$

where I is the average moment of inertia of the molecule and D_R is the rotational diffusion constant.

The relevant quantities to compare with the simulations are the Fourier transforms

$$S_l(\omega) = \frac{1}{\pi} \int_0^\infty F_l(t) \cos \omega t \, dt, \tag{17}$$

where the condition $F_l(0) = 1$ implies that the integral of $S_l(\omega)$ must be unity. The resulting expression is thus

$$S_l(\omega) = \frac{H}{\tau_0 + \tau_1} \text{Re}\left[\frac{A\tau_0 + B\tau_1 + 2AB}{1 - \frac{AB}{\tau_0 \tau_1}}\right], \tag{18}$$

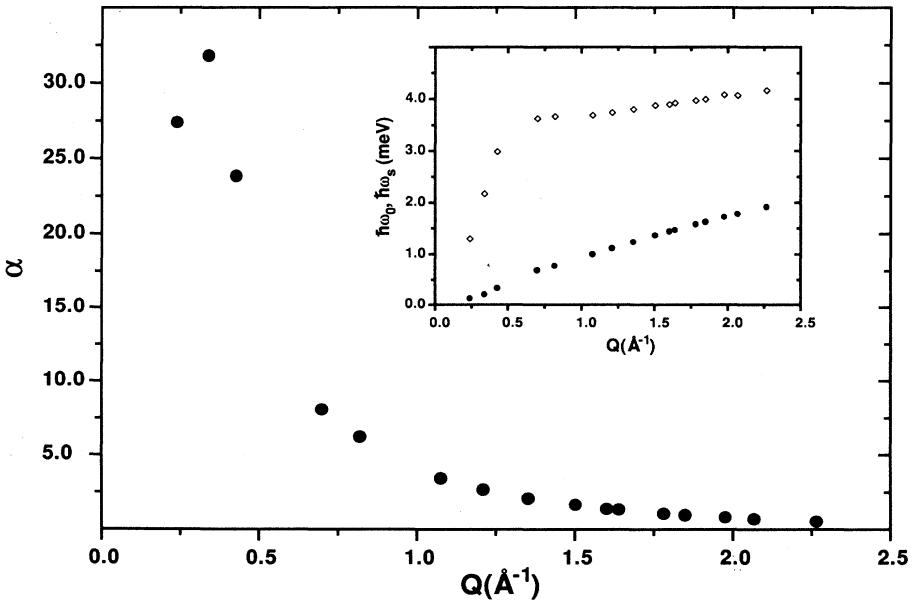

FIG. 3. Calculated values for the α parameter to assess the shape of the self-scattering function. The inset shows ω_0 (full circles) and ω_s (hollow circles). See the text for details.

TABLE II. Parameters describing the rotational relaxation functions (see the text).

Parameter	$S_1(\omega)$	$S_2(\omega)$
τ_0 (ps)	1.08	1.44
τ_1 (ps)	1.24	0.77
D_R $(\text{ps})^{-1}$	0.18	0.17
I (amu Å^2)	16.08	17.02

where H is a normalization constant and

$$A_l = \sqrt{\frac{I\pi}{l(l+1)k_BT}}\exp\left[-\frac{I(\tau_0^{-2}+\omega^2)}{4l(l+1)k_BT}\right] \times \exp\left[i\frac{I\omega}{2l(l+1)k_BT\tau_0}\right], \quad (19)$$

$$B_l = \frac{2\left[l(l+1)D_R + \tau_1^{-1}\right]}{\omega^2 + \left[l(l+1)D_R + \tau^{-1}\right]^2}. \quad (20)$$

The fits were performed over simulation data corresponding to $S_1(\omega)$ and $S_2(\omega)$, at 230 K with the parameter set τ_0, τ_1, D_R, H, and I, and some representative results are summarized in Table II. Notice that the residence time in both rotational states is in agreement with the previous estimation that they are of the same order of magnitude [21].

In Fig. 4 we show the simulated and fitted curves for $S_1(\omega)$ and $S_2(\omega)$. Excellent agreement is seen for the first one, and although the second one shows some discrepancies at long times, the rotational diffusion constant from both are in good agreement with previously estimated values (cf. Ref. [21]) from NMR studies that range from 0.12 to 0.25 ps^{-1} in the 190–230 K temperature interval. The fitted average moments of inertia are within the minimum and maximum values along the principal axis for a free molecule [10] (8.35 and 57.15 amu Å^2, respectively).

C. Coherent scattering law

The time Fourier transform of the sum of $I_s(Q,t)$ and $I_d(Q,t)$ (i.e., the total scattering law) was evaluated from simulation data. The general shape of such a function is shown in Fig. 5 for three different Q values. As can be clearly seen from the graphs, finite-frequency excitations are clearly seen at the lowest wave vectors, indicating the presence of relatively well defined collective density oscillations. To account for the shape of this spectral component, recourse was again made to a three-pole approximation, which was supplemented by a Lorentzian quasielastic contribution, added in a heuristic way. A similar approach has been followed for other liquids [20], since no closed-form expression to model the coherent quasielastic response for a molecular liquid seems to be available. The expression thus reads

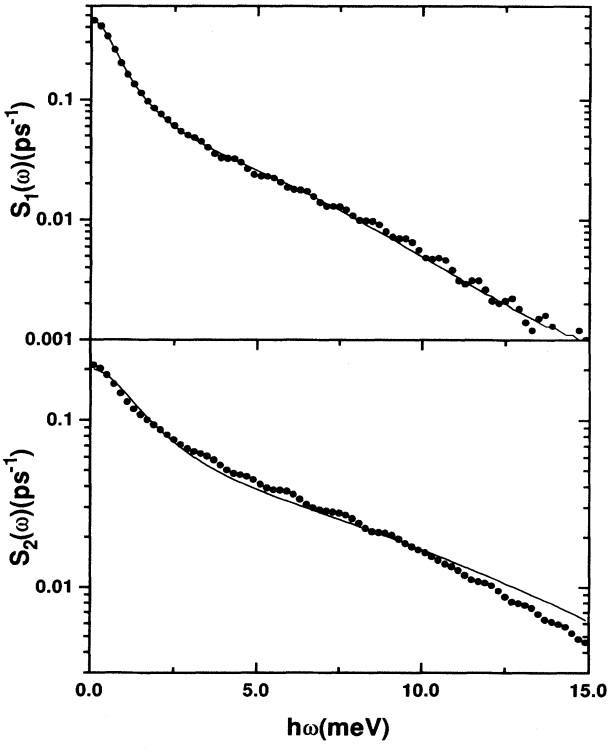

FIG. 4. Fourier transforms of the first two rotational relaxation functions obtained from the simulation (dots), compared with Larsson's model.

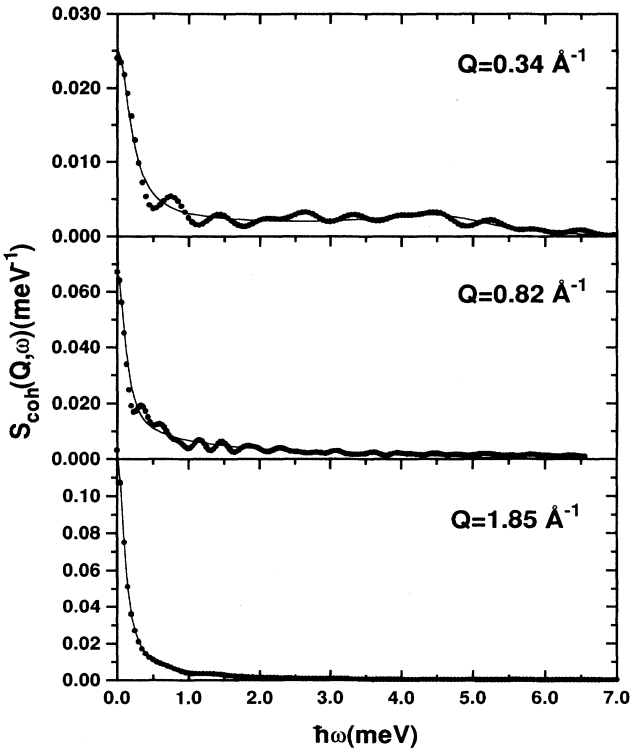

FIG. 5. Total coherent scattering function from simulation data, compared with the proposed three-pole plus a Lorentzian model.

$$S_{\rm coh}(Q,\omega) = C_1 \frac{\Gamma(Q)/2}{\omega^2 + [\Gamma(Q)/2]^2} + C_2 \frac{\tau\omega_0^2(\omega_l^2 - \omega_0^2)}{[\omega\tau(\omega^2 - \omega_l^2)]^2 + [(\omega^2 - \omega_0^2)]^2}, \quad (21)$$

where ω_0 and ω_l are the square roots of the reduced second and fourth frequency moments of the coherent dynamic structure factor, which encompass all the relevant information regarding the collective dynamics. Within a Maxwellian (viscoelastic) approximation, the relaxation time has the expression

$$\tau = \frac{\sqrt{\pi}}{2} \frac{1}{\sqrt{\omega_l^2 - \omega_0^2}}, \quad (22)$$

whereas the parameter $\Gamma(Q)$ has no clear physical meaning within the viscoelastic ansatz, although we will get some insight into its behavior. In Fig. 5 we show $S_{\rm coh}(Q,\omega)$, obtained from the simulations, compared with the model proposed in Eq. (21) for three different Q values. Apart from the high-frequency ripple arising from truncation effects, the model adopted here reproduces the spectral shapes in a satisfactory fashion. The information that results from such an analysis regards the even-frequency moments of the scattering law for coherent motion.

In Fig. 6 we show the calculated zeroth frequency moment $S(Q)$ as well as the fitted ω_0 and ω_l values. The slope of ω_0 vs Q for wave vectors approaching the hydrodynamic regime (below some 0.5 Å^{-1}) gives a value for the isothermal sound velocity of 1000 m s^{-1}, not too far from a previously reported value (1234 m s^{-1} at 210 K) [11]. Also, by a comparison of the data shown in Fig. 4 and those depicted in Fig. 3 of Ref. [11], notice that the rather flat shape of the "dispersion curve" found in the previous inelastic scattering experiment, which can be accounted for by the broad peak in $S(Q)$ (a double peak in the experimental magnitude [10]), is basically reproduced by the simulation results. The proposed model is based on the viscoelastic ansatz for the relaxation time in which the condition to support collective density oscillations is [23]

$$3\omega_0^2 > \omega_l^2, \quad (23)$$

which is manifested through the observed maxima at nonzero ω values. The condition set in Eq. (23) holds for wave vectors below 0.43 Å^{-1}. In Fig. 6 we also show the calculated $S(Q)$ and (in the inset), the $g(r)$ curves. The maximum at $Q \simeq 1.8$ Å^{-1} corresponds to a minimum in the ω_0 curve, which shows a small dip. Notice that the ideal gas limit of this frequency moment equals the second frequency moment of the self-scattering law and from Fig. 6 it may be seen that such a limit is indeed approached for momentum transfers above some 2 Å^{-1}. On the other hand, an estimate of the c_∞ high-frequency sound velocity can be readily obtained from the slope at low wave vectors of ω_l and gives 1610 m s^{-1}. Again, a comparison of data above some 1 Å^{-1} and the experimental estimates for the same magnitude shown in Fig. 3a of Ref. [11] reveals rather similar trends, especially the flat shape of ω_l for those wave vectors.

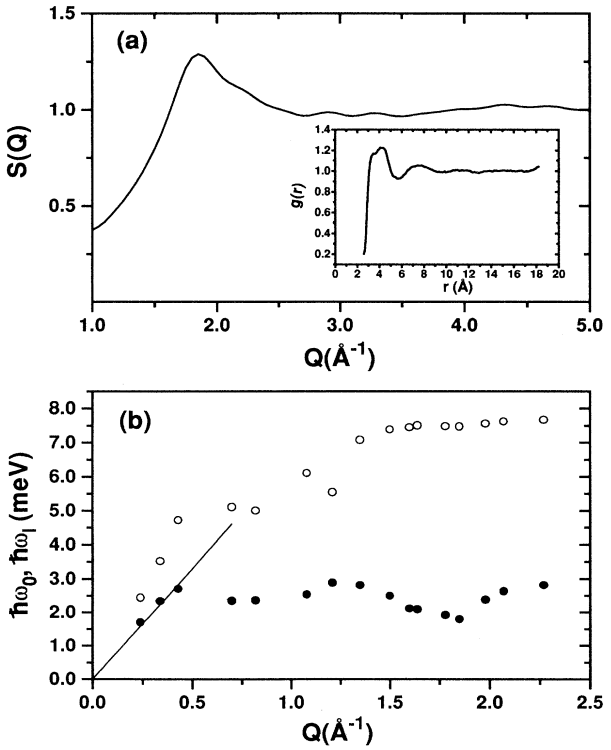

FIG. 6. (a) Static structure factor obtained from simulation. Inset: static pair correlation function. (b) Fitted ω_0 (filled circles) and ω_s (hollow circles) as a function of Q for the total coherent scattering function. The line shows the fitted slope for ω_0 at low-Q values to get an estimate of the sound velocity.

D. Molecular form factor

As stated above, the $F_2(Q)$ molecular form factor strongly depends upon the details of the orientational correlations between different molecules [cf. Eq. (6)]. In the case of complete randomness of the orientational degrees of freedom, its calculation is greatly simplified since

$$F_2(Q) = F_{2,u}(Q) = \left[\sum_\mu b_\mu \frac{\sin(Qr_\mu)}{Qr_\mu}\right]^2. \quad (24)$$

However, in our case with highly polar and nonspherical molecules, it is strongly suspected that such an hypothesis does not hold. It is then imperative to make a more complete calculation based on Eq. (6) for given distributions of orientation angles. Several models can be constructed for $F_2(Q)$ if information regarding the preferential orientation is available. To our knowledge, such an exercise only becomes practicable if some oversimplifying assumptions such as the existence of long-range orientational correlations are introduced. A more realistic treatment would rather consider the existence of such correlations within some correlation length R_c around the central molecule and a completely random distribution of orientations outside such a sphere. To achieve an

estimation of the most probable relative orientations between a pair of molecules, we employed pair correlation functions from numerical simulations and the results are briefly commented on in the next subsection.

E. Comparison with experimental data

Once the different motions have been taken into account, an approximate form for the dynamical structure factor can be derived. The strongest approximation in the expression that follows concerns the consideration of different movements as statistically independent since closed form expressions would be prohibitively involved otherwise. The quantity to be compared with experiment is therefore computed after introduction of all the required ingredients in Eq. (2) and a subsequent Fourier transform. The resulting total structure factor then reads

$$S(Q,\omega) = [S_{\rm coh}(Q,\omega) - S_{\rm self}(Q,\omega)]\, F_2(Q) + v_0(Q)\, S_{\rm self}(Q,\omega) + v_1(Q)\, \frac{1}{\pi}\int_{-\infty}^{\infty} d\omega' S_{\rm self}(Q,\omega') S_1(\omega-\omega') + v_2(Q)\, \frac{1}{\pi}\int_{-\infty}^{\infty} d\omega' S_{\rm self}(Q,\omega') S_2(\omega-\omega'), \tag{25}$$

where $S_{1,2}(\omega)$ are basically the time Fourier transforms of the rotational relaxation functions.

As stated above (cf. Sec. III A), the comparison between simulation and experiment required some fine tuning of some parameters, such as the self-diffusion coefficient [and all the other transport quantities related to it such as the relaxation time appearing in $I_s(Q,t)$; cf. Eq. (10)] for which the simulation provides rather low values, as well as some other parameters such as the $F_2(Q)$ structure factor or the width Γ of the coherent quasielastic spectrum entering Eq. (21), for which realistic models are difficult to build. These were taken as the only adjustable parameters against the experimental, constant-Q spectra and the agreement between simulation and experiment can be gauged from Fig. 7. The most interesting results regarding the fitted values for the molecular structure factor $F_2(Q)$ are shown in Fig. 8. As can be seen, the estimated structure factor is not far from that which corresponds to the case of uncorrelated molecular orientations up to momentum transfers of $Q \simeq 1.5$ Å^{-1}, whereas it approaches the curve calculated assuming a strong correlation of orientations from this value on. Such a curve was calculated from molecular geometries derived from the analysis of the partial $g_{\alpha\beta}(r)$ pair correlation functions calculated by means of Monte Carlo simulations. In fact, from maxima in $g_{\alpha\beta}(r)$ it was inferred that three different relative orientations were compatible with the simulated data and the model $F_2(Q)$ curve depicted in the figure corresponds to an average over the three configurations.

We can interpret this result on the basis that for low wave vectors we are exploring large regions in space, so

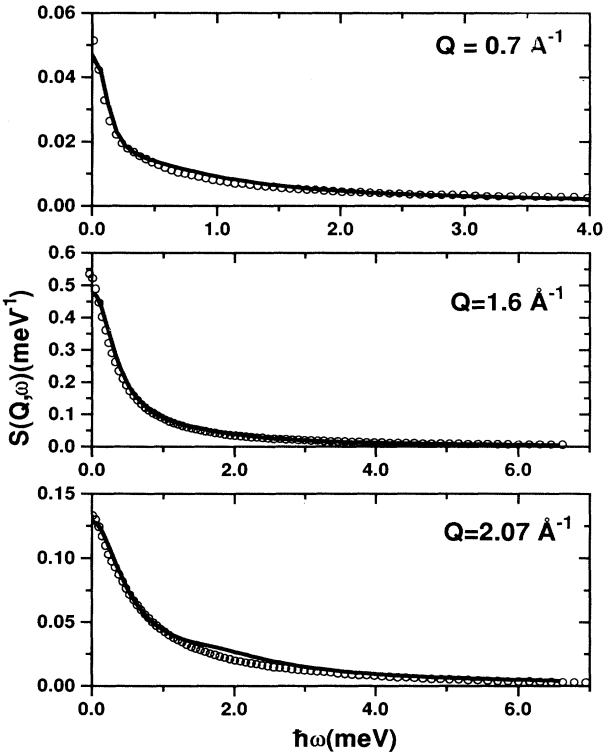

FIG. 7. Comparison between experimental neutron spectra (circles) and simulation results (solid line), for the wave vectors given in the inset.

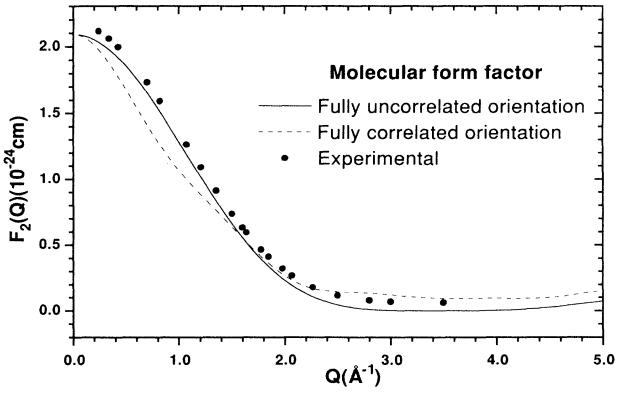

FIG. 8. Compared molecular form factors. The full line is the uncorrelated case, while dashed line indicates the correlated case obtained from three different configurations. Full circles indicate the molecular form factor fitted from the experimental data.

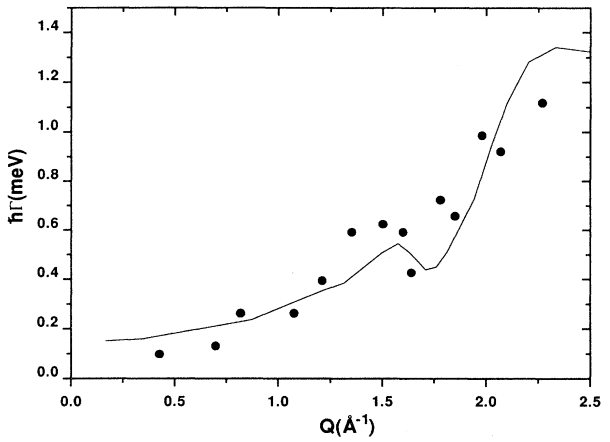

FIG. 9. Estimated width of the coherent quasielastic component to the spectra (circles). The solid line represents an approximation in terms of Eq. (26) using a value of 0.3 $Å^2$ ps^{-1} for the D_E Enskog self-diffusion coefficient and 3.5 Å for the σ_s hard sphere diameter.

the uncorrelated hypothesis is right through an average of a large number of configurations, whereas for larger Q's we are exploring the vicinity of a molecule, so the proposed pairwise configurations holds. An estimate for a lower bound to the correlation length could thus be carried from $R_c \approx 2\pi/Q_b$, where Q_b is taken as that corresponding to the change of behavior of $F_2(Q)$, $Q_b = 1.5$ $Å^{-1}$, which gives some 4.2 Å for R_c. Such a value is to be compared with some other estimates derived from the extent in real space where the experimental $g(r)$ shows some structure [10] that provides a value of approximately 10 Å, which should be taken as an absolute upper bound for this quantity.

It is also interesting to delve into the information provided by the wave vector dependence of the coherent quasielastic widths $\Gamma(Q)$. According to some kinetic theory results [24], such a quantity should vary as

$$\Gamma(Q) = \frac{D_E Q^2/S(Q)}{1 - j_0(Q\sigma_s) + 2j_2(Q\sigma_s)}, \tag{26}$$

where $D_E = k_B T/M\xi_E$ is the Enskog self-diffusion coefficient, which is expressible in terms of the temperature, molecular mass, drag factor ξ_E and σ_s, a hard-sphere diameter. A comparison between the values of $\Gamma(Q)$ derived from the interplay between simulation and experiment and those calculated from the equation given above using reasonable values for the two relevant parameters (i.e., $D_E = 3 \times 10^{-9}$ m^2 s^{-1} and $\sigma_s = 3.5$ Å) is shown in Fig. 9. Notice that both the magnitude and shape of $\Gamma(Q)$ are reproduced if the large statistical error in the data are accounted for. The value estimated for D_E is about 30% smaller than the actual self-diffusion coefficient, which is easily understood from results on hard sphere systems [25], which evidence a pronounced decrease in the quantity D_E/D for high-density fluids.

IV. DISCUSSION AND CONCLUSIONS

The present paper reports a quantitative attempt to analyze the dynamic correlations of a dense dipolar liquid in terms of well established semiphenomenological models to account for the single-particle and collective dynamics. In particular, the $I_s(Q,t)$ self-scattering law was successfully described through a three-pole model, which showed that the validity of the Fickian diffusion regime is confined below $Q \simeq 0.5$ $Å^{-1}$. The dynamics of molecular rotations was well described by a two-state model due to Larsson and Bergstedt [22] through the introduction of two characteristic times, corresponding to free rotational and diffusional regimes. A consistent value for the rotational diffusion constant was obtained independently from the first- and second-order relaxation functions, in good agreement with NMR data. On the other hand, some of the parameters derived from comparison between simulation and experiment, such as the coherent quasielastic widths, can be accounted for using realistic values for the relevant parameters, thus lending further support to the validity of the procedure followed here to analyze the experimental and computer simulation data.

From a comparison between simulation and experiment an estimate of the extent of strong intermolecular correlations have been obtained. The characteristic distance $R_c \approx 4.2$ Å indicates that for length scales covering the first coordination shell the orientational correlations are remarkably strong and these die away in a rather smooth fashion up to some 10 Å. With the present data at hand, it becomes difficult to assess whether the decay of orientational correlations follow any prespecified form [i.e., proportional to $\exp(-r^2/R_c^2)$ or any other simple form] and it is not even clear that something significant can be gained from experimental diffraction data of higher accuracy [10]. However, by comparison with other well studied cases [15] it seems clear that the most significant difference between this liquid and others formed by particles interacting mainly via dispersion forces concerns the clear change of behavior of the $F_2(Q)$ structure factors at wave vectors not far from those characteristic of the first peak in $S(Q)$.

A comparison between the present results and some recent reports stating the existence of long-ranged orientational order in dipolar fluids [9] (i.e., a ferroelectric nematic phase) seems in order. The thermodynamic state of the system here explored corresponds, using the same reduced units as employed by Groh and Dietrich [9], to that of a fluid composed of dipoles of aspect ratio $k = 6.87$ and dipole moment $m^* = 1.13$ at a reduced temperature $T^* = 0.68$ and density $\rho^* = 0.7$ [27]. An inspection of the phase diagrams given in Ref. [9] for systems not too far from that considered here ($m^* = 1, k = \infty$) places the state point analyzed here well within the instability region (i.e., according to the calculation, the isotropic liquid would be stable for temperatures about 1.7 times the actual one). On the other hand, entrance into the ferroelectric phase would require an increase in density of some 1.3 times the actual one for the liquid with a concomitant increase in temperature of some 1.2

times. Consideration of the compressibility and volume expansion of the liquid [28] shows that such a state could possibly be achieved by an increase in temperature up to some 300 K and an applied pressure of the order of 3 kbar.

From the simulation data, the hydrodynamic limits of the dielectric functions $\epsilon'(\omega)$,$\epsilon''(\omega)$ were calculated as Fourier-Laplace transforms of the autocorrelation functions for the fluctuations of the total dipole moment. The calculated curves from the model of rigid dipoles used for the present simulation show a broad maximum in $\epsilon''(\omega)$ centered at approximately 4 meV, which is somewhat below the maximum of the experimental generalized frequency distribution (see, for instance, Fig. 3a of Ref. [12] for plots of this quantity) and a change in sign of $\epsilon'(\omega)$ appearing at some 4.5 meV. Notice that a simple estimate of the frequency of this dipolar plasmon excitation from [1]

$$\omega_p^2 = \frac{4\pi N\mu^2}{VI^*\epsilon_\infty} \tag{27}$$

for liquid sulphur dioxide under the present conditions gives 6.5 meV, some seven times smaller than estimates for liquid water, understandable from the considerably smaller moment of inertia (I^*) and higher dipole density (N/V) and dipole moment (μ) of the former liquid. From the present data regarding the molecular dynamics, we can reassess the condition of existence of "dipolaron" oscillations. This can be written in a simplified form as [7]

$$\epsilon(0)\epsilon(\infty) \geq \omega_s^2\tau_s\tau_D/4, \tag{28}$$

where $\epsilon(0,\infty)$ are the zero- and infinite-frequency permitivities (taken as 17.6 and 1.99, respectively [26]), ω_s is the free (inertial) reorientational angular frequency, $\omega_s^2 = 2k_BT/I$, with I being the average moment of inertia, τ_D is the rotational diffusion time (both values obtained in Sec. III B), and $\tau_s = \tau_D[2\epsilon(0)+1]/3\epsilon(0)$. The left-hand side of Eq. (28) thus gives 35.02 and the right-hand side 6.25, so the stated condition regarding the existence of the oscillation holds. Therefore, such a collective mode should, if it exists, be visible in the high-frequency dielectric response $\epsilon(Q,\omega)$ measured by optical means (i.e., reflectivity at normal incidence) as a well defined peak located not far from some 4–6 meV.

Finally, it is worth emphasizing the fact that the most remarkable anomaly regarding the dynamics of this liquid, apart from the relatively large value for the molecular mass derived from analysis of $I_s(Q,t)$, concerns its reorientational movements, which substantially depart from simple exponential relaxation. Whether this can be interpreted as a clear manifestation of strong non-Markovian effects introduced by dielectric friction as claimed by some [29] or is just a simple consequence of geometrical constraints can be decided only after future experiments evidencing the presence of long-time tails in the orientational relaxation functions.

ACKNOWLEDGMENTS

Dr. M. Garcia-Hernandez and Dr. F.J. Mompean are acknowledged for the help given during the experimental measurements. This work was supported in part by Grant No. PB92-0114-c03-01 (Spain). J.D. wishes to thank CONICET (Argentina) and CSIC (Spain) for financial support. This work was performed in part at the Institut Laue-Langevin, Grenoble, France.

[1] R. Lobo, J.E. Robinson, and S. Rodriguez, J. Chem. Phys. **59**, 5992 (1973).
[2] E.L. Pollock and B.J. Alder, Phys. Rev. Lett. **46**, 950 (1981).
[3] A. Chandra and B. Bagchi, J. Chem. Phys. **92**, 6833 (1990).
[4] L.A. Davalos-Orozco and L.F. del Castillo, J. Chem. Phys. **96**, 9102 (1992).
[5] H.J. Kroh and B.U. Felderhof, Z. Phys. B **66**, 1 (1987). An attempt to reduce the problem of the dielectric friction of a rotating dipole to the continuum limit is reported by B. Bagchi and G.V. Vijayadamodar, J. Chem. Phys. **98**, 3351 (1993).
[6] A recent calculation showing the presence of a dipolaron peak in the dielectric response of liquid water is given by S.H. Kim, G. Vignale, and B. De Facio, Phys. Rev. E **50**, 4618 (1994).
[7] P. Madden and D. Kivelson, *Advances in Chemical Physics* (Wiley, New York, 1984), Vol. 56, p. 467.
[8] J.J. Weis and D. Levesque, Phys. Rev. E **48**, 3728 (1993).
[9] B. Groh and S. Dietrich, Phys. Rev. Lett. **72**, 2422 (1994), and references therein; see also H. Zhang and M. Widom, Phys. Rev. E **49**, R3591 (1994); Phys. Rev. Lett. **74**, 2616 (1995), and the ensuing response.
[10] M. Alvarez, F.J. Bermejo, P. Chieux, E. Enciso, M. García Hernández, N. García, and J. Alonso, Mol. Phys. **66**, 397 (1989).
[11] J.L. Martinez, F.J. Bermejo, M. Garcia-Hernandez, F.J. Mompean, E. Enciso, and D. Martin, J. Phys. Condens. Matter **3**, 4075 (1991).
[12] A. Chahid, M. Garcia-Hernandez, C. Prieto, F.J. Bermejo, E. Enciso, and J.L. Martinez, Mol. Phys. **78**, 821 (1993).
[13] F. Sokolić, Y. Guissani, and B. Guillot, Mol. Phys. **56**, 239 (1985).
[14] N. G. Almarza (unpublished). An attempt to refine the potential was done using different sets of parameters and comparing the results of Monte Carlo calculations with the experimental $g(r)$ pair correlation function. No substantial improvement in the overall performance of the potential used in the present report was found.
[15] P.A. Egelstaff, D.I. Page, and J.G. Powles, Mol. Phys. **20**, 881 (1971).
[16] V.F. Sears, Can. J. Phys. **44**, 1279 (1966).
[17] S.W. Lovesey, J. Phys. C **6**, 1856 (1973).
[18] M. Gerl, in *Amorphous Solids and the Liquid State*, edited by N.H. March, R.A. Street, and M. Tosi (Plenum, New York, 1985).

[19] M.F. Collins and W. Marshall, Proc. Phys. Soc. **92**, 390 (1967).

[20] F.J. Bermejo, F. Batallán, J.L. Martinez, M. García Hernández, and E. Enciso, J. Phys. Condens. Matter **2**, 6659 (1990). For a review containing quasielastic scattering data for a variety of liquid systems see F.J. Bermejo, A. Chahid, M. Garcia-Hernandez, J.L. Martinez, F.J. Mompean, W.S. Howells, and E. Enciso, Physica B **182**, 289 (1992); for inelastic scattering see F.J. Bermejo, A. Chahid, A. Criado, J.L. Martinez, M. García-Hernández, and F.J. Mompean, J. Mol. Struc. **296**, 295 (1993).

[21] R.E. Wasylishen, J.B. Macdonald, and J.O. Friedrich, Can. J. Chem. **62**, 1181 (1984).

[22] K.E. Larsson and L. Bergstedt, Phys. Rev. **151**, 117 (1966).

[23] S.W. Lovesey, in *Theory of Neutron Scattering from Condensed Matter* (Oxford Science, New York, 1986), p. 213.

[24] I.M. de Schepper, E.G.D. Cohen, and M.J. Zuilhof, Phys. Lett. A **101**, 399 (1984).

[25] P.A. Madden in *Liquids, Freezing and the Glass Transition*, Proceedings of the Les Houches Summer School of Theoretical Physics, Session LI, edited by J.P. Hansen, D. Levesque, and J. Zinn-Justin (North-Holland, Amsterdam, 1991), p. 548.

[26] *International Critical Tables* (McGraw-Hill, New York, 1926), Vol. 1.

[27] The estimates for the effective values for the Lennard-Jones (LJ) parameters $\epsilon^{\text{eff}}/k_B = 340$ K, σ^{eff}=3.6 Å were taken by scaling down the values given by Sokolić *et al.* [13] for a Stockmayer fluid by an amount that decreases the values of a three-center LJ model upon consideration of point charges [i.e., the effective molecular diameter comes quite close to the estimate for the hard-sphere Enskog fluid (3.5 Å)].

[28] S. Miskiewicz, K. Rieser, and T. Dorfmüller, Ber. Bunsen. Phys. Chem. **80**, 395 (1976).

[29] C.V. Vijayadamodar and B. Bagchi, J. Chem. Phys. **95**, 5289 (1991).